Bond capacity of grid system in unresin carbon fiber reinforcement for concrete beams

Rudy DJAMALUDDIN*, Shinichi HINO** and Kohei YAMAGUCHI***

* Dr.Eng., Research Fellow, Dept. of Civil Engineering, Kyushu University, Fukuoka
** Dr.Eng., Professor, Dept. of Civil Engineering, Kyushu University, Fukuoka
*** Dr.Eng., Research Associate, Dept. of Civil Engineering, Kyushu University, Fukuoka

The unresin continuous carbon fiber (UCCF) cable has a disadvantageous point as low bond capacity to the concrete. In order to improve bond action between the UCCF cable and concrete, a grid system has been developed. This paper presents an experimental study on mechanical performance of the developed grid system. The following tests were conducted: pullout test and flexural test. Furthermore, a model of the grid system is proposed for evaluation of its bond capacity. The result of pullout test indicated that the specimen with 5 units of grid had ten times bond capacity compared to the adhesive bond capacity of the cable itself. On the flexural test, the grid offered a good effect in which the beam with grid system showed similar failure mode with the concrete beam reinforced by steel bar. Finally, the proposed model was used to predict the grid bond capacity of the experimental results.

Key Words: *Grid, Bond capacity, Carbon fiber, Pullout, Concrete beam, Failure mode*

1. Introduction

Recently, some innovative uncorrosive materials such as carbon, aramid and glass fibers have been introduced as reinforcements for concrete structures. They have advantages over conventional steel reinforcement in specific applications such as concrete structures in corrosive environments, where electrical or electromagnetic insulation is required, or when high strength-to-weight ratio is desired[1].

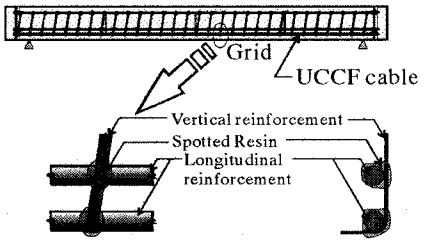

Figure 1 Grid System

Regarding to the attempts to utilize the fiber materials effectively, a new method in utilizing the unresin carbon fibers as reinforcement for concrete structures has been introduced. This method is called Un-resin Carbon-fibers Assembly System (UCAS). UCAS has been developed not only for the unresin carbon fibers reinforcing system (UCCF:Unresin Continuous Carbon Fiber) but also for the resin carbon fiber reinforcing system (CFRP: Carbon Fiber Reinforced Plastics). The reinforcement is assembled by turning the carbon fiber string between two end-anchors under certain constant tensile force both when preparing the unresin or resin reinforcement system[2]. The disadvantageous point of UCCF cable is the low adhesive bond capacity to concrete.

As reinforcing materials for a concrete structure, bond capacity of UCCF cable becomes an important factor to

Table 1 List of the Test Specimens

Test	Specimen		Main cable	Vertical		Dimension (mm)			Expected
	Type	Name	(strand)	Cable (strand)	Pitch (mm)	Width	Height	Depth/Span	failure mode
Pullout test	1	G-0*)	2 x 40	5	50	125	250	300	Bond slip failure on grid
	2	G-1*)							
	3	G-3*)							
	4	G-5*)							
Flexural test	A	RC-SN	3-D10	No	None	100	140	550	Shear failure
	B	CF-SN	52	No					
	C	CF-G		12	50				
	D	CF-Gs							

*) Three specimens for each type

sustain an effective flexural action. In UCAS , a grid system has been developed to improve the bond capacity. The detail of grid system is illustrated in Figure 1. The grid system is manufactured by connecting a pair of longitudinal reinforcement with vertical reinforcement using epoxy resin adhesive.

This paper presents an experimental study on mechanical performance of the grid system. The following tests were conducted: pullout test and flexural test. The pullout test is aimed to obtain the grid bond capacity as well as the adhesive bond capacity of cable itself. A series of concrete beams were also manufactured and tested to clarify the performance of grid on concrete beams. Finally, a model of the grid system is proposed for evaluation of its bond capacity.

2. Experimental Procedure

To reach the goal of this study, four types of pullout test specimens and four beam specimens as shown in Table 1 were manufactured and tested for pullout and flexural tests, respectively. For the pullout test, three specimens for each type were prepared. Details of pullout test specimens are presented in Figure 2(a). These specimens were made from concrete block with dimension of 125 x 250 x 300 mm and a pair of embedded cables. Specimen type 1, 2, 3 and 4 were specimens with no grid (G-0), one grid (G-1), three grids (G-3) and five grids (G-5), respectively. Strain gauges were attached along the cable of one specimen (specimen No.3) of each type to measure the strain distribution. The grid was provided by connecting a pair of main cable made of 40 strands of carbon fibers and vertical cable made of 5 strands of carbon fibers using epoxy resin. The specimens were tested under loading system presented in Figure 2(b).

Figure 3 shows the details of beam specimen. Four specimens with a clear span of 550 mm and cross section of 100 by 140 mm were manufactured. These beams were designed to fail under shear. Type A was the specimen reinforced with three D10 steel deformed bars without stirrup, while type B, C, and D were specimens reinforced with UCCF cables without grid, with grid and with grid plus additional spotted resin, respectively. The specimen type A was manufactured as a control specimen to show that the beam with a good bond would fail as be predicted. The specimen type D was manufactured to investigate the effect of additional spotted resin to the flexural behavior. The design capacity of the beam specimens are presented in Table 2. It should be noted here that those design capacities are calculated under assumption that there is a perfect bond between reinforcement and concrete. The concrete beam

Table 2 Design Capacity of Beam Specimens

Beam Reinforced by	Flexural load (kN)		Shear cracking load (kN)	Failure mode
	Pcr	Pu		
Steel (RC-SN)	20.17	77.5	55.7	Shear failure
UCCF cables (CF-SN, CF-G, CF-Gs)	20.17	159.8	51.6	Shear failure

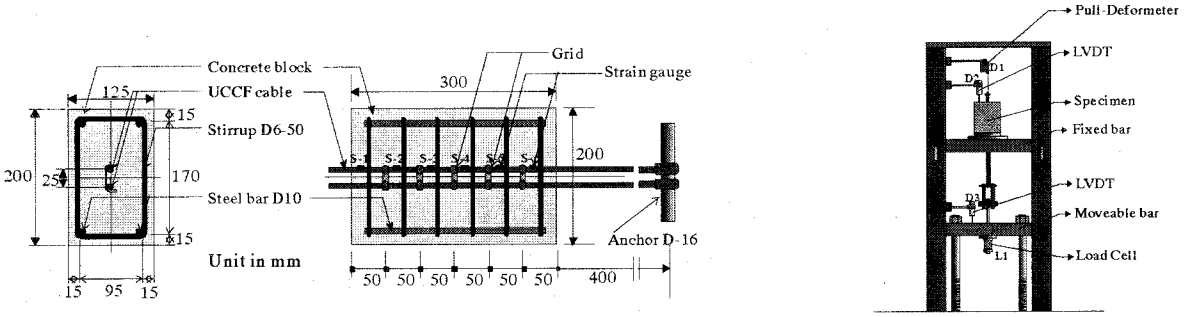

(a) Specimen Detail (b) Test Setup

Figure 2 Specimen Detail and Test Setup for Pullout Test

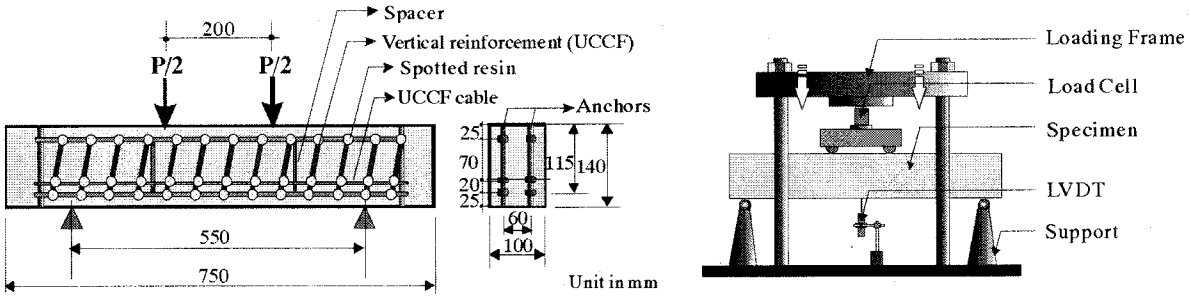

(a) Specimen Detail (b) Test Setup

Figure 3 Specimen Detail and Test Setup for Flexural Test

specimens were tested under loading system as shown in Figure 3(b).

The material properties of concrete for pullout and beam specimens, carbon fiber (Torayca T700S-12K) and resin are presented in Table 3. Tensile properties of carbon fiber was the properties of carbon fiber string provided by manufacturer, not for carbon fibers cable. Experimental test showed that the tensile strength of cable was approximately 35% of the strength of carbon fiber string itself. It was assumed that the cable failed when the cable reached the tensile strength of 1680 MPa[2].

2.1. Pullout Test Results

(1) Adhesive Bond Capacity

The summary of experimental result for specimen without grid (G-0) is presented in Table 4. The contact surface area of cables to the concrete and bond strength are also shown in the table. The results showed that the UCCF cables had very low bond strength. If it is compared to the bond strength of the coated steel deformed bar[3], UCCF cable has bond strength approximately only 1/15 of the coated steel deformed bar.

Figure 4(a) shows the load-slip relationship of specimen without grid (G-0), while Figure 4(b) shows its strain distribution (specimen G-0-3). From the load-slip relationship, generally, it can be considered that the load-slip response is linear up to the maximum point. This response is different from load- slip response of carbon fiber reinforced plastic (CFRP) bar, where it was reported that the load-slip response of CFRP bar was bilinear[4]. In the unresin carbon fiber cable, when load was given, the free-end slip increased simultaneously under linear response until the cable reached its maximum bond capacity. From here, the load decreased near to zero followed by the increasing of free-end slip.

The recorded strain in cables of specimen type G-0 was distributed as shown in Figure 4(b). S-1 was a point near to the free-end while the point S-6 was a point nearest to the loading point (see Figure 2(a)). Initially, the strain was distributed from small on S-1 to large on S-6. When the maximum bond capacity was reached, the strain on S-4, S-5 and S-6 decreased. From here, the strain of S-1 and S-3 little increased while the strain S-4, S-5 and S-6 decreased. This indicated that the bond had lost and the strain on cables was going to be redistributed uniformly along the cables.

Table 3 Material Properties

Material Name	Strength (MPa)			Young's modulus (GPa)	Density (gr/cm^3)	Cross sectional area (mm^2)
	Tensile	Compressive	Shear			
Torayca T700S-12K*)	4800	-	-	230	1.82	0.46
Steel D10	300	300	-	200	7.80	78.5
Epoxy Resin*)	53.0	95.9	12.7	3.40	-	-
Concrete for Pull-Out	5.40	72.0	-	43.4	2.40	-
Concrete for Beam	2.69	40.4	-	31.6	2.40	-

*) Provided by manufacturer

Table 4 Bond Strength of UCCF Cables

No.	Specimen type	Specimen name	Maximum point		Cable diameter (D) (mm)	Bonding area (Ab) (mm^2)	Bond strength (fb) (MPa)
			$Pmax$ (kN)	Slip (S) (mm)			
1	G-0	G-0-1	3.43	1.90	6.16	5803	0.30
2		G-0-2	2.55	1.01	6.16	5803	0.22
3		G-0-3	3.04	1.80	6.16	5803	0.26

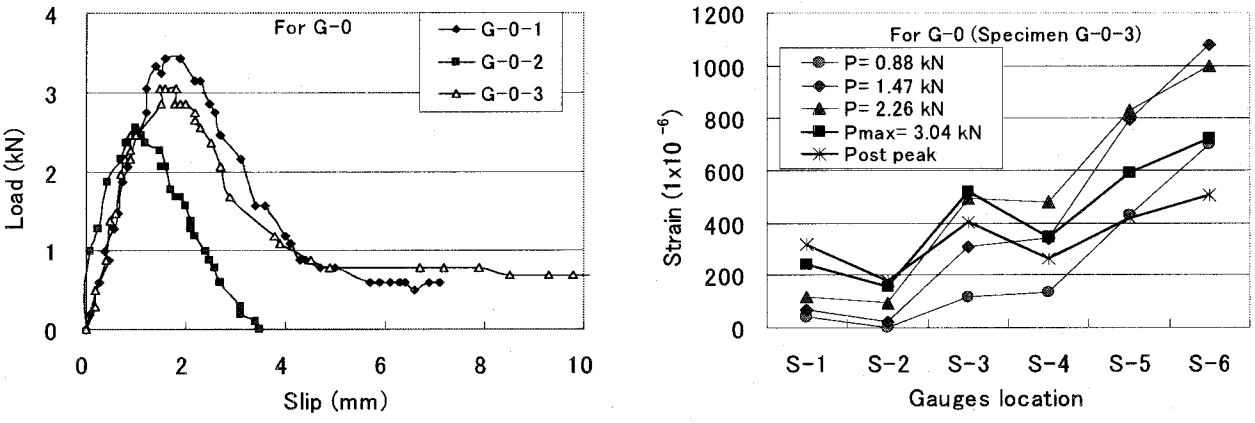

(a) Load - Slip Relationship

(b) Strain Distribution

Figure 4 Load - Slip Relationship and Strain Distribution of Specimen G-0

(2) Experimental Grid Bond Capacity

The load-slip relationship and strain distribution of specimens with grid are presented in Figures 5 to 7, respectively. Generally, the load-slip response of these specimens were almost linear up to the maximum load. All specimens had similar load-slip relationship where, initially, the load and slip increased simultaneously until the peak load. When the maximum capacity was reached, the load dropped and it was followed by the increasing of free-end slip. Some of specimens showed suddenly dropping. It should be explained here that since the fibers are bundled together to form a cable, it will has a deformable section area. When embedding it within concrete, the geometry of cable may be changed and the cement paste may infiltrate in different way between each specimen into the cable. Due to this phenomenon and the low bond capacity of the embedded cable, it is difficult to avoid the dispersion of experimental data as it has been measured on the specimen G-0 (Figure 4(a)) and specimen G-1 (Figure 5(a)). Even though, as the number of grids was increased, the total load

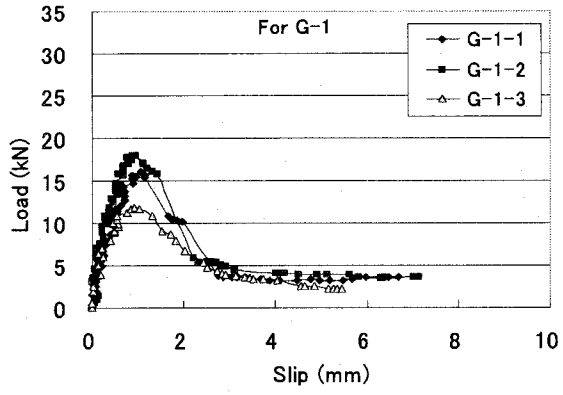

(a) Load - Slip Relationship

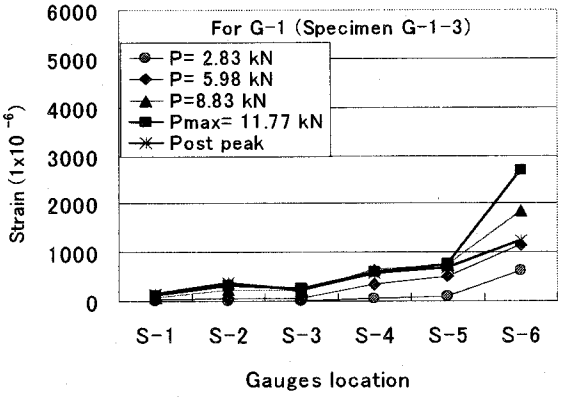

(b) Strain Distribution

Figure 5 Load - Slip Relationship and Strain Distribution of Specimen G-1

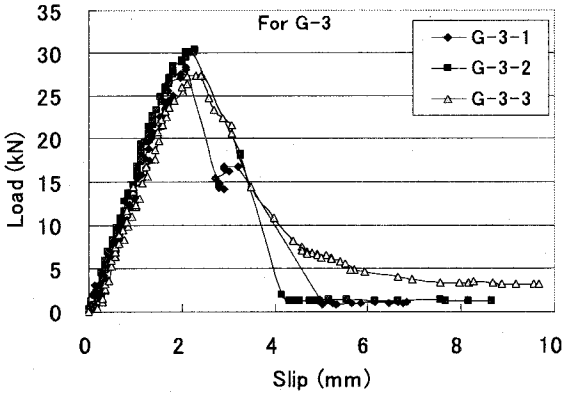

(a) Load - Slip Relationship

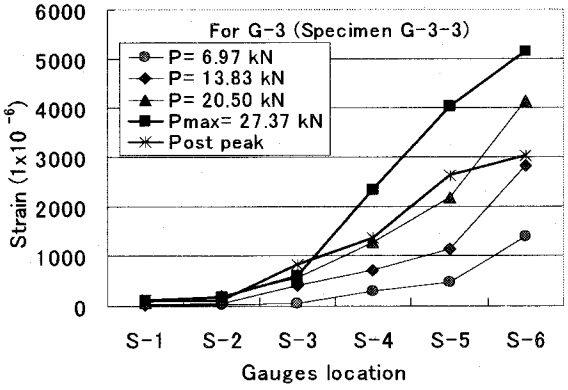

(b) Strain Distribution

Figure 6 Load - Slip Relationship and Strain Distribution of Specimen G-3

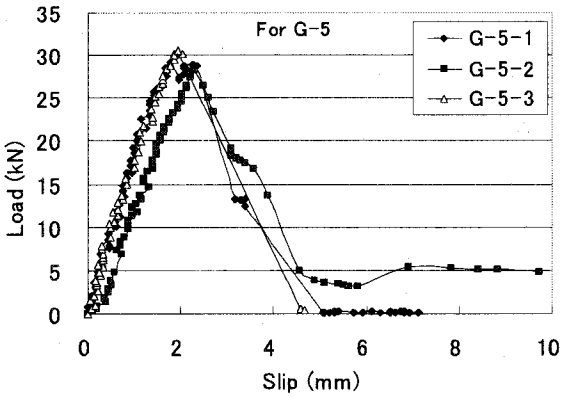

(a) Load - Slip Relationship

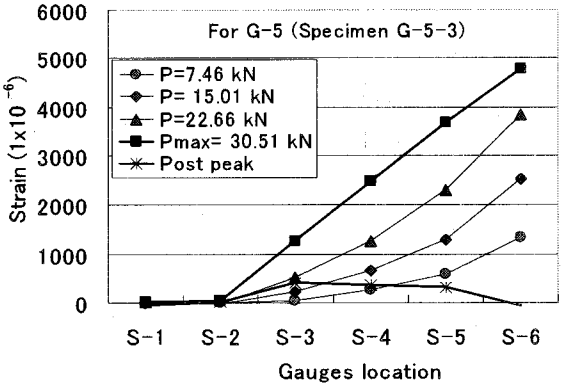

(b) Strain Distribution

Figure 7 Load - Slip Relationship and Strain Distribution of Specimen G-5

increased. As the results, the effect of bond capacity became smaller. This reduced the dispersion of data as it was found on the specimens G-3(Figure 6(a)) and G-5 (Figure 7(a)).

Based on the recorded strain in the cables, the results indicated that the strain was distributed from approximately zero on S-1 to maximum on S-6. For specimen G-1, the strain on S-6 indicated that the cable on that point sustaining maximum tensile forces among the other points. This was caused by the existing of a grid in which the grid sustained a portion of the tensile load and transferred them to the concrete. The strain on the section without grid was just influenced by the adhesive bond of the cables itself.

Table 5 presents the summary of pullout test results. Results indicated that the pullout loads increased by increasing the number of grids. However, it was found that almost there was no significant increasing in pullout load of the specimen G-5 compared to the specimen G-3. This can be clearly observed through Figure 8 that shows the diagram bar of maximum load of all specimens. The equivalent performance of specimen with 3 grids (G-3) and 5 grids (G-5) indicates that the effective number of grids in sustaining tensile load is 3 or 4 grids. Mechanically, on the specimen G-5, the first grid failed before grid No.4 or No.5 fully sustained the load. The failure of the first grid caused the next grids to fail simultaneously in a second. As the result, the total load of specimen G-5 was not affected by all grids but by the first 3 grids.

Figure 9 shows the average maximum capacity to show the effectiveness of the grid. The figure shows that the adhesive bond capacity of cable without grid (G-0) was about 10% of specimen with 5 grids. If the adhesive bond capacity of cable was about 1/15 of the coated steel bar then it can be also considered that the specimen with 5 grids has about 2/3 of bond capacity of the coated steel bar.

2.2 Flexural Test Results

(1) Load-Deflection Relationship

Experimental load-deflection relationship of the tested beam specimens are shown in Figure 10 and Figure 11. Figure 10 indicates the comparison of the load-deflection relationship of specimen RC-SN and specimen CF-SN. While in Figure 11, the beams with grid-system (CF-G and CF-Gs) are compared with CF-SN beam. Initially, all the beams were uncracked and stiffened. With further loading, cracks occurred at mid-span when the applied moment exceeded the cracking moment *Mcr*, causing a reduction in stiffness, which was greater in beam reinforced with UCCF cables than in the RC beam. This can be attributed to the fact that crack openings were wider and crack spacings narrower in CF-SN than in RC-SN. Figure 11 shows that, after cracking, the beams reinforced with UCCF cables have almost the same stiffness.

On the CF-SN beam, with further loading, a mid-span crack widened and propagated fast upward near the top of compression side. This single crack continued to widen until the concrete started to crush when the applied load reached 92.7 kN. From here the load increased and it was followed by the crushing of concrete until the load reached 124.4 kN. With further loading, the load started to decrease which

Table 5 Bond Capacity of the Grid

No.	Specimen type	Specimen name	Specimen characteristics	Maximum point				Ratio to adhesive bond (average)*)
				P max (kN)		Slip (mm)		
					Average		Average	
1	G-1	G-1-1	1 units of grid	15.99	15.27	1.06	0.98	5.08
2		G-1-2		18.05		0.97		
3		G-1-3		11.77		0.93		
4	G-3	G-3-1	3 units of grid	28.35	28.71	2.08	2.25	9.55
5		G-3-2		30.41		2.27		
6		G-3-3		27.37		2.42		
7	G-5	G-5-1	5 units of grid	29.14	29.33	1.78	2.01	9.76
8		G-5-2		28.35		2.30		
9		G-5-3		30.51		1.95		

*) See Table 4

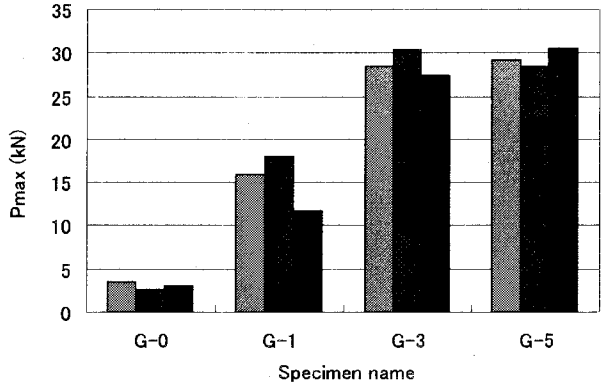

Figure 8 Maximum Capacity

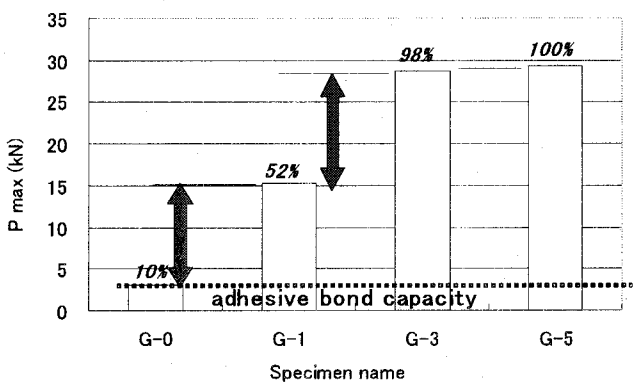

Figure 9 Efectiveness of Grid

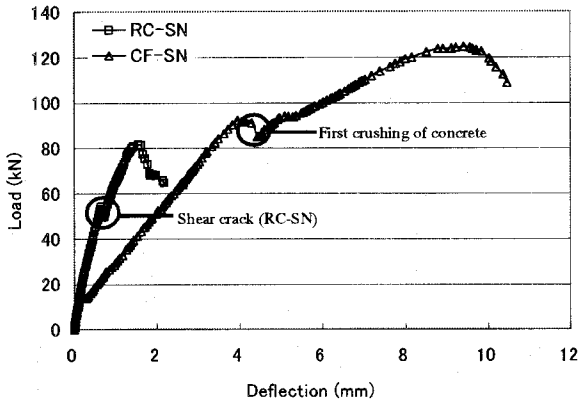

Figure 10 Load-Deflection Relationship of RC-SN and CF-SN

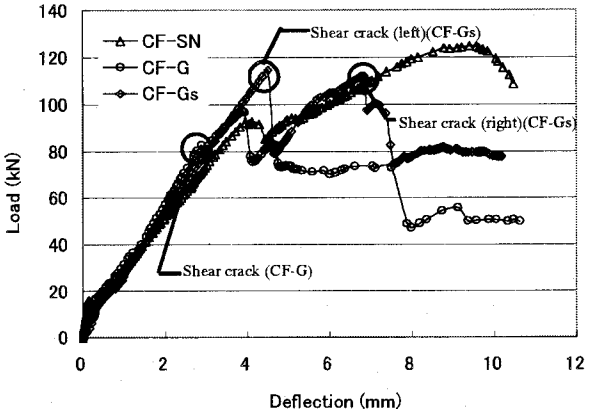

Figure 11 Load-Deflection Relationship of CF-SN, CF-G and CF-Gs

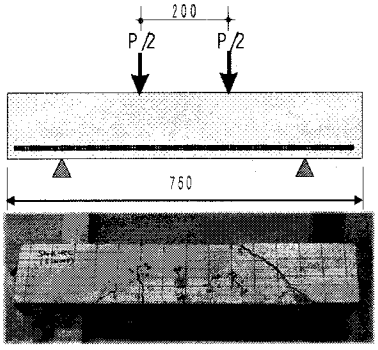

Figure 12 RC-SN

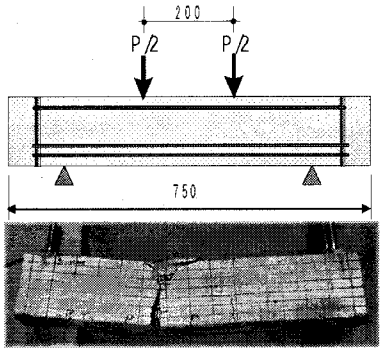

Figure 13 CF-SN

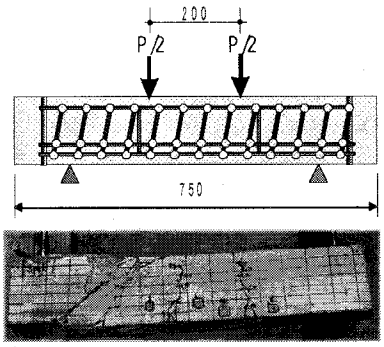

Figure 14 CF-G

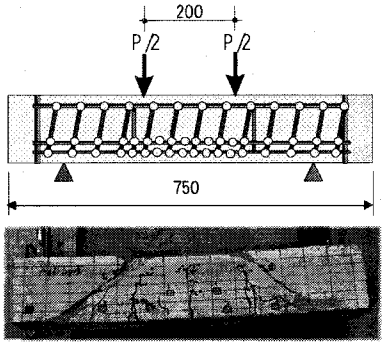

Figure 15 CF-Gs

was followed by increasing of deflection until the end of test.

The propagating of single crack on CF-SN may be attributed to the fact that carbon fiber cable could not be bond perfectly to the surrounding concrete. While on the RC-SN beam, after crack occurred on the center-span, the cracks continued to widen and propagated upward. With further loading, an inclined crack occurred when load reached 50 kN and the load little decreased. This crack propagated from the support to the loading point on the right side. This was caused by the fact that the beam did not has shear reinforcement. The shear forces were just sustained by the concrete. From this point, the load still increased and it was followed with the widening of the inclined crack until about 80 kN and then load decreased and beam failed. The single crack did not occur on the RC-SN beam. This may be attributed to the fact that they had much bond capacity between steel bar and concrete, so that its flexural capacity was higher than its shear capacity without stirrups.

By providing the grids along the UCCF cable of specimens CF-G and CF-Gs, the flexural behavior was similar to the RC-SN, that is the flexural cracks initially propagated and they were followed by shear cracking when the applied load reached about 80 kN on specimen CF-G and 110 kN on specimen CF-Gs, respectively. The dispersion of flexural performance between specimen CF-G and CF-Gs may be caused by the additional spotted resin between grids. Regarding to the effect of additional spotted resin to the flexural behavior, a further study should be done.

(2) Failure Mode

Figures 12 to 15 show the failure mode photographs of tested beam specimens. As it was designed, the steel concrete beam without stirrups failed under shear failure. This may be attributed to the fact that the steel had high bond capacity to concrete. On the beam reinforced with UCCF cables without grid (Figure 13), the beam failed under single flexural cracking. This was attributed to the fact that the UCCF cables had low adhesive bond capacity to concrete so that the beam could not develope an effective flexural action. By providing the grids as it had been applied to the specimen CF-G (Figure 14), the flexural capacity of beam increased and so that why the beam failed under shear failure similar to the beam reinforced by steel bar (Figure

14). On the last beam (Figure 15), some additional spotted resins were provided to increase the bond capacity of reinforcement. The result shows that the beam also failed under shear cracking on both sides.

3. Model of the Grid

Bond stresses cause the stress or force in a tensile reinforcement on a concrete beam changes from point to point along the length of the reinforcement[5]. In case of grid system, by ignoring the adhesive and friction forces, the stress or force changes from one grid segment to the next grid segment. This can be illustrated by the free body diagram presented in Figure 16. If T_B is greater than T_A, the grid force Fg must act on the intersection point of the grid to maintain the equilibrium. Summing forces parallel to the reinforcement direction, the grid force Fg will be:

$$F_g = T_B - T_A \quad (1)$$

where :
F_g : Grid force (N)
T_A : Tensile force in segment A (N)
T_B : Tensile force in segment B (N)

If ε is the strain in cable and Ae, Ecf are the effective cross sectional area and Young's modulus of cable, respectively, then the tensile force in each segment can be expressed with Eq.(2). The effective section area of the UCCF cable is approximately 75% of the total section area[6].

$$T = A_e \times E_{cf} \times \varepsilon \quad (2)$$

where:
T : Tensile force occurred in reinforcement (N)
Ae : Effective cross sectional area of the cables (mm^2)
E_{cf} : Young's modulus of UCCF (N/mm^2)
ε : Strain in cable

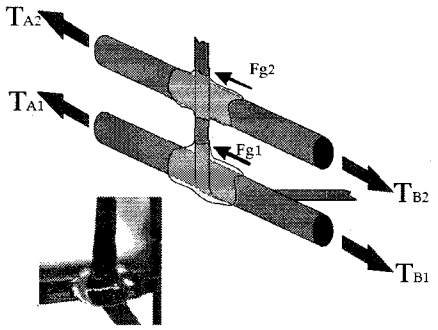

Figure 16 Illustration of Grid Force

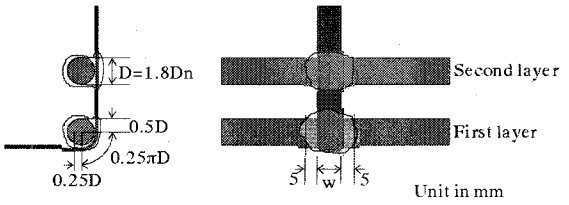

Figure 17 Grid Bond Surface Model

Bond capacity Fg is affected by some factors such as: grid bond surface (contact area), shear strength of epoxy, stress in the vertical reinforcement, concrete strength, etc. Between those factors, the shear strength of epoxy and the contact area are the most important factors in predicting the bond capacity of the grid. Based on consideration and for simplification of the model, only shear strength of epoxy and grid bond surface have been used in the model of grid system. There are two types of surfaces of a grid that may be formed in constructing the grid by using the intersection between vertical reinforcement and longitudinal reinforcement. The first one is the curved-grid (first layer intersection) and the second one is the normal crossed grid (second layer grid). The bond surface area of both types are illustrated in Figure 17. The bond surface areas of the first and the second layer intersections may be expressed as follows:

$$A_{b1} = 1.8D_n(0.75 + 0.25\pi)(w + 10) \quad (3(a))$$
$$A_{b2} = 1.8D_n(w + 10) \quad (3(b))$$

where :
A_{b1} : Bond surface area of the first layer intersection (mm^2)
A_{b2} : Bond surface area of the second layer intersection (mm^2)
w : Width of the vertical reinforcement (taken as 5 times of the diameter of the bundled fibers for vertical reinforcement which is calculated by using the individual section area of strand) (mm)
D_n : Diameter of the cable calculated by using the individual section area of the strand (mm).
$= \sqrt{(4nA_{cf})/\pi}$, (n : Number of strand per cable, A_{cf}: Section area of UCCF strand)

So, the grid bond capacity of the grid may be predicted using :

$$F_{b1} = A_{b1} \times \tau_e \quad (4(a))$$
$$F_{b2} = A_{b2} \times \tau_e \quad (4(b))$$

where :
F_{b1} : Grid bond capacity of the first layer intersection (N)
F_{b2} : Grid bond capacity of the second layer intersection (N)

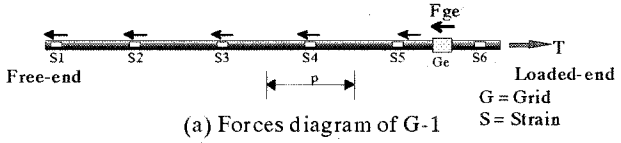

(a) Forces diagram of G-1

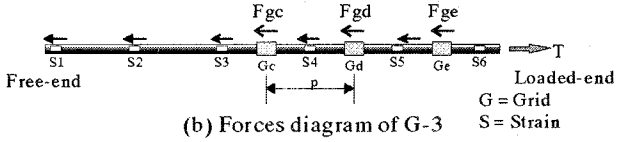

(b) Forces diagram of G-3

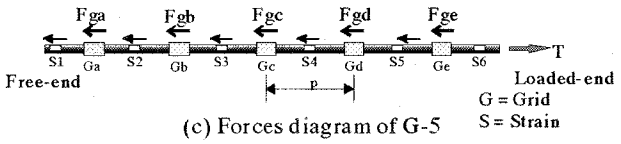

(c) Forces diagram of G-5

Figure 18 Free-Body Diagram

Table 6 Grid Force of Model vs Experiment

Grid No.	Name	Experimental Grid Forces *Fg**)			Predicted Grid Bond Capacity *Fb* (N)
		Fg for G-1(N)	*Fg* for G-3 (N)	*Fg* for G-5 (N)	
1	*Fge*	3730	3174	3089	3153
2	*Fgd*	-	4802	3369	
3	*Fgc*	-	4872	3450	
4	*Fgb*	-	-	3434	
5	*Fga*	-	-	42 **)	
Average		3730	4283	3336	
Fg/Fb		1.18	1.36	1.06	

*) The sectional area of cable is the effective sectional area.
**) Not used in average value

τ_e : Shear strength of the epoxy resin (N/mm^2) (provided by manufacturer, see Table 3)

It should be noticed here that the grid in the pullout test was provided by using the first type surface. Figure 18 shows the free body diagram of the pullout specimens. By using the Eq.(2) and Eq.(4), the experimental grid force as well as the predicted grid bond capacity are presented in Table 6. The experimental *Fgd* and *Fgc* of G-3 were little higher than the others. This may be attributed to the fact that the grid surface on that point was wider than the model. However, the average results show that there was a good agreement between the predicted results and the experimental results. The average experimental bond capacity was approximately 20% higher than the predicted bond capacity.

It should be added here that the proposed model was developed only for the proposed grid system of UCCF cable to predict the bond capacity of the grid when the UCCF cables were applied as tensile reinforcement in a concrete beam. As it was explained before that for simplification, the grid model was developed by considering only the effect of the epoxy shear strength and the grid bond surface, however, more useful model considering another parameters such as concrete strengths should be established in the further study.

4. Conclusions

Based on the test result and discussion, the major conclusions may be summarized as follows :

(1) Bond strength of the UCCF cable was very small. If it was compared to the bond strength of coated steel deformed bar, UCCF cable had only 1/15 of bond strength of coated steel deformed bar.

(2) The proposed grid system developed good mechanical bonding effect between cable and concrete. On the specimen with 5 units of grid, the bond capacity increased approximately ten times compared to the adhesive bond capacity of cable.

(3) The beam without grid system failed under single flexural crack while the specimens with grid system failed under shear failure.

(4) Grid system can be used to develop a mechanically bonding effect between reinforcement and concrete. Due to the existing of the grid system on reinforcement, the effective reinforcing action between reinforcement and concrete may be achieved. This will lead to reducing of crack spacing and crack width.

The proposed preliminary model could be used to evaluate the bond capacity of the grid system. However, to establish the more useful model considering another parameters such as concrete strengths, a further study should be done.

Acknowledgment

This research was conducted at the Structural and Aesthetic Design Laboratory of Kyushu University under cooperation with the Intelligent Machinery Laboratory of Kyushu University. The financial support of Japan Society for the Promotion of Science (JSPS) in this research program is gratefully acknowledged.

References

1) A. Nanni: Flexural Behavior and Design of RC Members Using FRP Reinforcement, Journal of Structural Engineering, Vol.119, No.11, pp.3344-3359, November 1993.

2) R.Djamaluddin, T.Ohta, K.Yamaguchi, and K.Harada: Fundamental Study on Application of UCAS to Concrete Structures, Proceedings of a Joint Research Symposium in Combination with the COE International Workshop, Fukuoka, pp.30-35, January 2002.

3) R.A.Treece and J.O.Jirsa: Bond Strength of Epoxy-Coated Reinforcing Bars, *ACI Material Journal*, V.86, No.2, pp.167-174, March-April 1989.

4) T.Nagahama, I.Kuroda, D.Rudy, S.Hino and T.Ohta: Bond-Slip Behavior of Two Dimensional Carbon Fiber-Reinforced Plastic Grids, Memoirs of the Graduate School of Engineering Kyushu University, V.59, No.2, 1999,pp.93-105.

5) J.G.MacGregor: Reinforced Concrete Mechanics and Design, Prentice Hall, 1998.

6) R.Djamaluddin: Fundamental Study on Application of Unresin Continuous Carbon Fiber Reinforcing System to Concrete Structures, Doctor dissertation of Faculty of Engineering, Kyushu University, 2003.

(Received September 12, 2003)